POLYMER-CLAY NANO BRICK WALLS FOR TRANSPARENT GAS BARRIER ON PLASTIC FILM

Morgan A. Priolo, Graduate Research Assistant, Texas A&M University, College Station, TX
You-Hao Yang, Graduate Research Assistant, Texas A&M University, College Station, TX
Jaime C. Grunlan, Assistant Professor, Texas A&M University, College Station, TX.

Abstract

Layer-by-layer (LbL) assembly is a thin film deposition technique capable of creating thin, multifunctional coatings from water based mixtures. LbL films, typically < 1μm thick, are created by alternately exposing a substrate to mixtures of positively- and negatively-charged species. This deposition process is repeated until the desired number of "bilayers" (or cationic-anionic pairs) is achieved. Assemblies of natural sodium montmorillonite clay, polyethylenimine, and poly(acrylic acid) that are only 51 nm thick, have been produced with an oxygen transmission rate (OTR) below 0.005 $cm^3 \cdot m^{-2} \cdot day^{-1}$ (permeability two orders of magnitude lower than SiOx when OTR multiplied by thickness), believed to be due to a nano brick wall structure. These thin, transparent composites, which can contain up to 80 wt. % clay, are a good candidate for foil replacement in food packaging and flexible electronics packaging. All-polymer coatings containing polyethylenimine and poly(acrylic acid) are also shown to exhibit an undetectably low OTR after only 10 bilayers are deposited. All of the coatings described are created from water-based solutions and fabrication occurs under ambient conditions. By changing the deposition materials used, these films can also be made to exhibit a tacky behavior, which may be useful for pressure sensitive tapes.

1. Introduction

A variety of functional thin films can be produced using the layer-by-layer (LbL) assembly technique [1, 2]. LbL-based thin films are currently being evaluated for a variety of applications that include anitmicrobial [3, 4], molecular sensing [5], solid battery electrolyte [6], photovoltaics [7], membranes [8], anti-fungal [9], electrical conductivity [10] , and flame retardance [11, 12]. Thin films, typically < 1μm thick, are created by alternately exposing a substrate to positively- and negatively-charged molecules, polymers, or particles, as shown in Figure 1. In this case, steps 1 – 4 are continuously repeated until the desired number of "bilayers" (or cationic-anionic pairs of layers) is achieved. Each individual layer may be 1 – 100+ nm thick depending on chemistry, molecular weight, charge density, temperature, deposition time, counterion, and pH of species being deposited. The ability to control coating thickness down to the nm-level, easily insert variable thin layers without altering the process, avoid disturbing intrinsic mechanical behavior of the substrate, and process under ambient conditions are some of the key advantages of this deposition technique. These films often have properties that are better than comparable thick films (>>1μm). Furthermore, these films are often transparent, which opens up areas of use not available to comparable bulk films. Altering the order and composition of layers provides limitless opportunity for new functionality. The clay-filled film shown schematically in Figure 1(b) is transparent, has excellent oxygen barrier, and is a basis for the work described here.

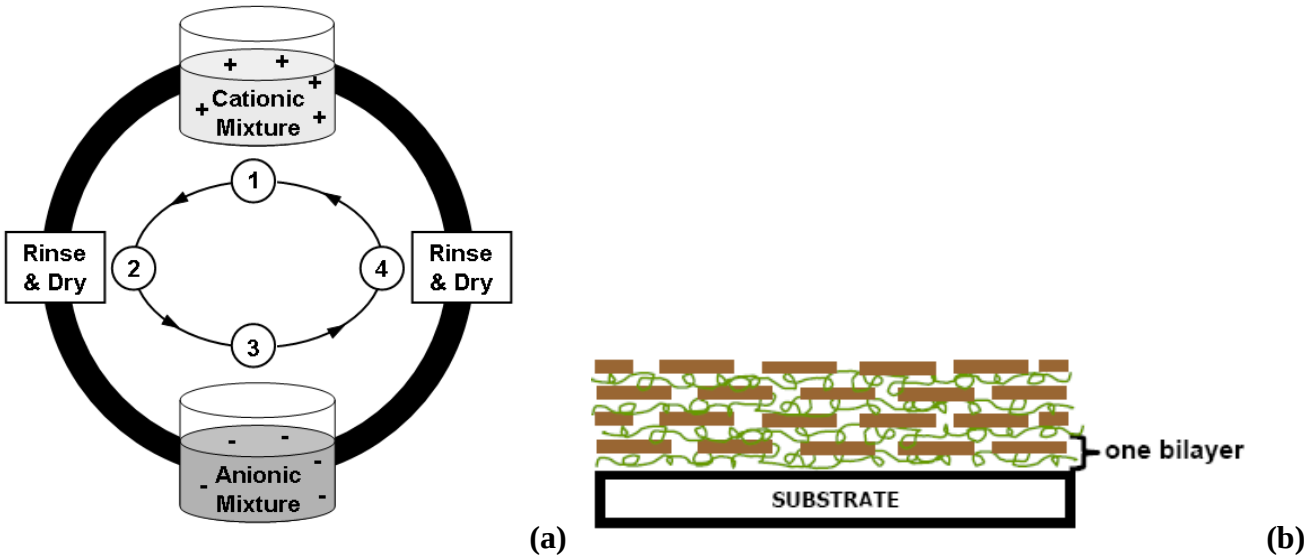

Figure 1. Schematic of the layer-by-layer self-assembly procedure for creating multifunctional thin films (a). Steps 1 – 4 are repeated to create a multilayer coating (b). This schematic is showing negatively-charged clay deposited with a polycation, which generates a nano brick wall structure.

2. Experimental

2.1 Materials

Cationic branched polyethylenimine (PEI) (M_w = 25,000 g/mol and M_n = 10,000 g/mol), anionic poly(acrylic acid) (PAA), and glutaraldehyde (GA) were purchased from Sigma-Aldrich (Milwaukee, WI). The pH of 0.1 wt. % PEI in deionized water and 0.2 wt. % PAA were adjusted using 1 M HCl and 1 M NaOH, respectively, prior to film assembly. A 1.0 wt. % solution of GA was used as a post-assembly room-temperature crosslinking agent. Southern Clay Products, Inc. (Gonzales, TX) supplied natural, untreated montmorillonite (MMT) (tradename Cloisite NA^+), and the pH of MMT suspensions were unaltered. This clay has a reported cationic exchange capacity of 0.926meq/g and is negatively-charged in deionized water. MMT platelets have a reported density of 2.86 g/cm^3, diameter of 10-1000nm, and thickness of 1nm [13]. Poly(ethylene terephthalate) (PET) film with a thickness of 179μm (trade name ST505, produced by DuPont-Teijin) was purchased from Tekra (New Berlin, WI) and used as the model substrate for OTR testing. This PET film has an OTR of approximately 8.6 cm^3/(m^2·day·atm) under dry conditions. Prior to coating, PET film was rinsed with deionized water, methanol, and again with water before being dried with filtered air. These substrates were then corona treated using a BD-20C Corona Treater (Electro-Technic Products, Inc., Chicago) to impart a negative surface charge [14, 15]. Single-side-polished silicon wafers (University Wafers, South Boston, MA), 500μm in thickness, were used for film growth characterization by ellipsometry. For deposition onto silicon wafers, a 30–minute piranha treatment was performed [16]. [***Caution***: Piranha solution reacts violently with organic materials and should be handled with extreme caution.] Following treatment, substrates were initially dipped in the PEI solution for 5 minutes, followed by rinsing with de-ionized water and blow drying with filtered air. The same procedure was followed with the clay suspension, or PAA solution, to complete the first bilayer. Each subsequent layer was dipped for one minute in each given aqueous mixture. Films with more than 10-bilayers and all films deposited onto PET for OTR testing were produced using home-built robots [17, 18].

2.3 Characterization

All films created for oxygen transmission rate testing were sent to MOCON (Minneapolis, MN) and tested in accordance with ASTM D-3985 [19], using an Oxtran 2/21 ML instrument. OTR testing was done at 23°C and 0%RH, unless otherwise specified. Film thickness was measured on silicon wafers using a PHE-101 Discrete Wavelength Ellipsometer (Microphotonics, Allentown, PA) at a wavelength of 632.8 nm and a 65° incidence angle. Thin film cross sections were imaged using a JEOL 1200EX TEM (Parody, MA). Weight of each deposited layer was measured with a MAXTEX quartz crystal microbalance (QCM) and 5 MHz gold-electrode quartz crystals. The quartz crystals were cleaned with an oxygen plasma etcher. Absorbance and transmittance of deposited films on fused quartz slides were measured with a USB2000 UV-Vis spectrometer (Ocean Optics).

3. Results and Discussion

3.1 Oxygen Barrier of PEI-MMT Assemblies

Figure 2 shows how the OTR of PEI-MMT films, deposited on PET, decreases with increasing space between clay layers [20]. Altering the clay spacing was achieved by simply altering the pH of the PEI deposition solution, which alters the polymer's charge density. At low pH, or in this case pH 7, PEI is highly charged and deposits thinner (due to self-repulsion of polymer chains) than when it is weakly charged at higher pH (pH 10). A cross-sectional TEM image (Figure 2 inset) clearly shows the orientation and structure of a PEI/MMT film. This 40-bilayer film, made with pH 10 PEI and MMT clay, shows every individual clay layer, explicitly proving the proposed nano brick wall structure in Figure 1. This barrier structure is most effective when appropriate clay spacing is achieved, which is evidenced by the dramatic decreases in OTR seen from pH 8 to pH 9 PEI and from pH 9 to pH 10 PEI. Also, polystyrene film was used as the substrate for TEM imagery because it sections better in the microtome.

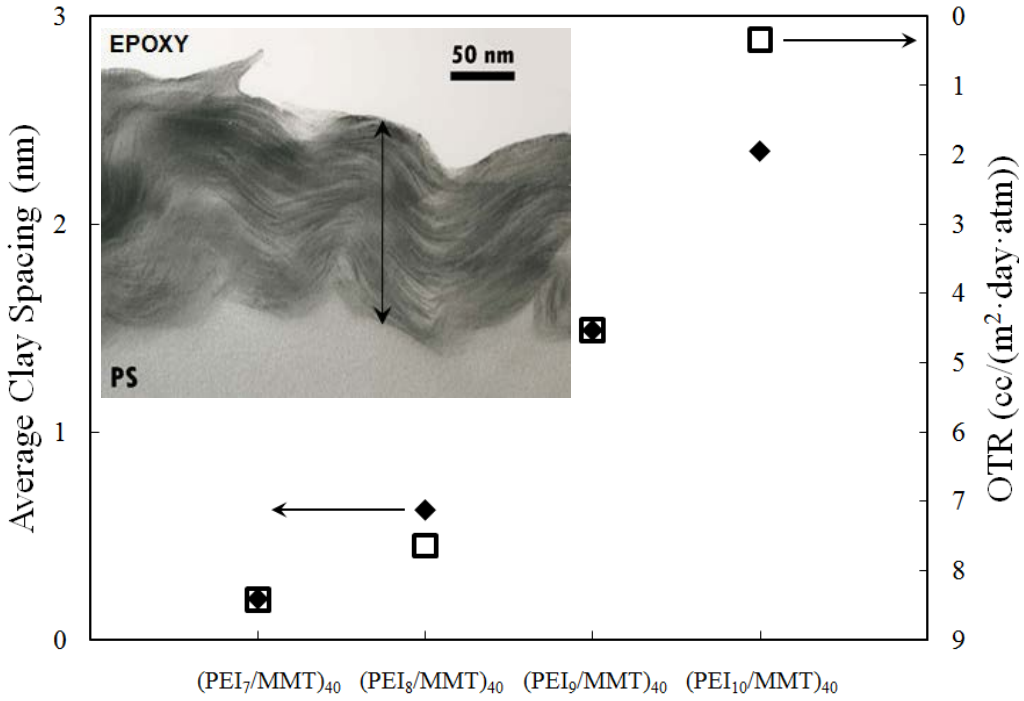

Figure 2. Oxygen transmission rate and average clay spacing as a function of PEI pH. Inset shows TEM cross-section of LbL film, containing 40-bilayers of clay and pH 10 polyethylenimine (from Ref. [20]).

3.1 Oxygen Barrier of Quadlayer Assemblies

With increasing thickness between clay layers having been shown to improve barrier performance in LbL assemblies [20], three polymer layers were deposited between each clay layer (i.e., a quadlayer [QL]) to further reduce OTR. Figure 3 reveals that both film growth and mass deposited of this QL assembly increases exponentially with layers deposited, with clay mass deposition remaining constant for each layer. By depositing these three polymer layers (PEI/PAA/PEI) between each clay layer, average clay spacing of greater than 10 nm can be easily achieved with only 4 clay layers. QCM also reveals that a 4QL film has a clay concentration around 37 wt. % [21]. This clay concentration is still far above that found in bulk composites, but shows much better optical transparency, clay organization, and barrier properties (at a thickness around 50 nm). This expansion of clay layers is a very effective barrier on PET, as shown in Figure 4. After only four clay layers are deposited (i.e., 4 QL), the resulting thin film has an oxygen transmission rate at the detection limit of commercial instrumentation (~ 0.005 $cm^3 \cdot m^{-2} \cdot day^{-1}$). When OTR is multiplied by thickness, this coating is shown to exhibit the lowest oxygen permeability ever reported for a polymer-clay material (< 5×10-22 $cm^3(STP) \cdot cm/(cm^2 \cdot s \cdot Pa)$), which is at least two orders of magnitude below that reported for completely inorganic SiOx barrier thin films [22-24] and four orders of magnitude lower than a 25 μm EVOH copolymer film [25]. This incredible barrier is due to the highly tortuous path permeating molecules must traverse, as theorized by Cussler [26]. Because the deposited clay platelets lie with their largest dimension parallel to the substrate (as seen in insets of Figure 2 and Figure 4), permeating molecules are forced to travel around the platelets and through the polymer layers perpendicular to the diffusion direction. This extended length is only realized when films exhibit clay spacing much greater than the kinetic diameter of diatomic oxygen, dk = 0.346 nm,[27] as shown in Figure 2. This level of clay spacing is easily achieved with this quadlayer film, with an average clay spacing of approximately 12nm for a 4QL film (assuming individual platelet deposition).

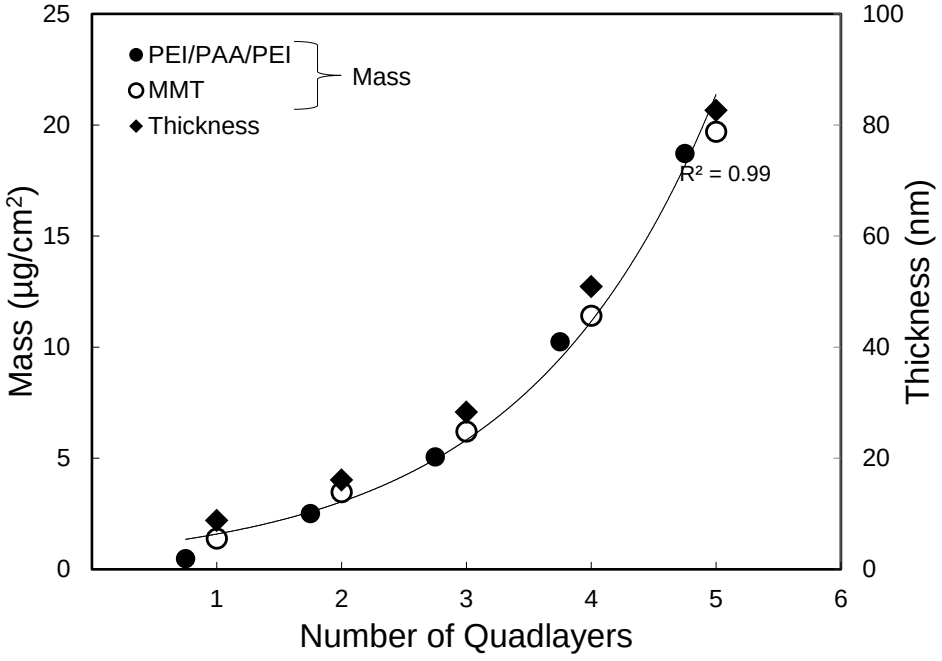

Figure 3. Mass and thickness as a function of quadlayers of PEI/PAA/PEI/MMT deposited (adapted from Ref. [21]). Thickness measurements were made using an ellipsometer with silicon wafer substrates and mass measurements were made using a quartz crystal microbalance.

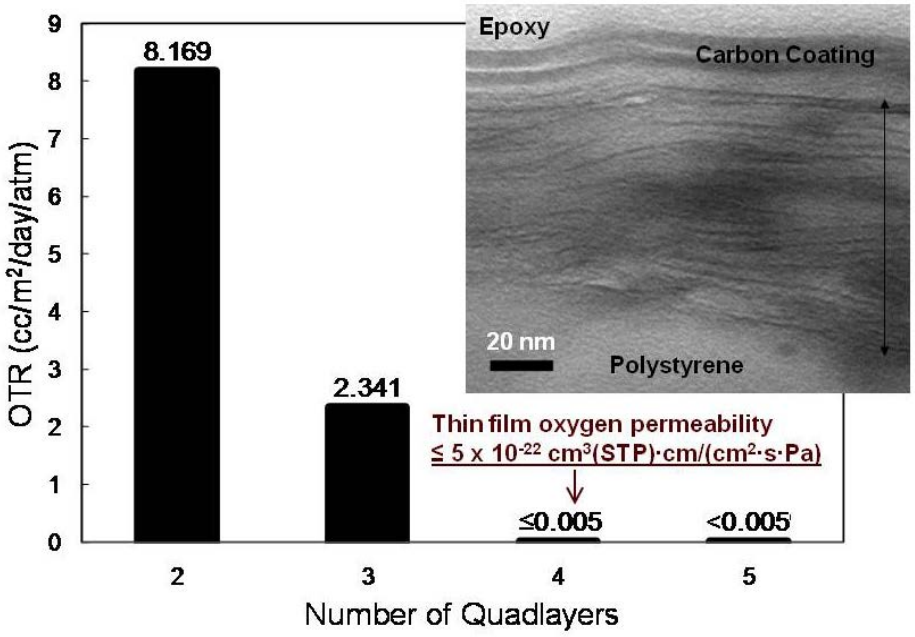

Figure 4. Oxygen transmission rate as a function of PEI/PAA/PEI/MMT quadlayers deposited on 7-mil PET (from Ref. [21]). The inset is a TEM cross-section of a 5 QL thin film. The double arrow spans the film's 80 nm thickness.

3.1 Oxygen Barrier of All-Polymer Assemblies

Thin film assemblies of branched polyethylenimine (PEI) and poly(acrylic acid) (PAA), deposited using the layer-by-layer technique, were studied in an effort to produce all-polymer thin films with low oxygen permeability [28]. Figure 5 reveals that altering the pH of PEI and PAA results in large thickness variations (from 90 nm to 4.74 μm for 30 bilayer films). Also, crosslinking these films with glutaraldyhyde (GA) creates an inhibition of polymer interdiffusion, causing exponential film growth to be reset when crosslinking occurs during film growth, rather than as a post-assembly treatment (see Figure 5 inset). As shown in Table 1, a crosslinked 8-bilayer film of PEI at pH10 and PAA at pH4 produces a 305 nm thick film with an oxygen transmission rate below 0.005 $cm^3 \cdot m^{-2} \cdot day^{-1}$ under dry conditions (PO_2 < 3.2×10-21 $cm^3(STP) \cdot cm \cdot cm^{-2} \cdot s^{-1} \cdot Pa^{-1}$). This permeability is the lowest ever reported for an all-polymer material, is three orders of magnitude lower than that of a 25 μm EVOH copolymer film [25], and an order of magnitude lower than all-inorganic SiOx thin films [23, 24, 29]. Even at 100% RH, this unique film maintains an OTR (0.09 $cc \cdot m^{-2} \cdot day^{-1}$) that is two orders of magnitude lower than that of the 7-mil PET substrate. Remarkably, a 10 BL film (~ 1 μm thick) is able to maintain an undetectably low barrier (OTR < 0.005 $cm^3 \cdot m^{-2} \cdot day^{-1}$) at 100%RH without need for crosslinking.

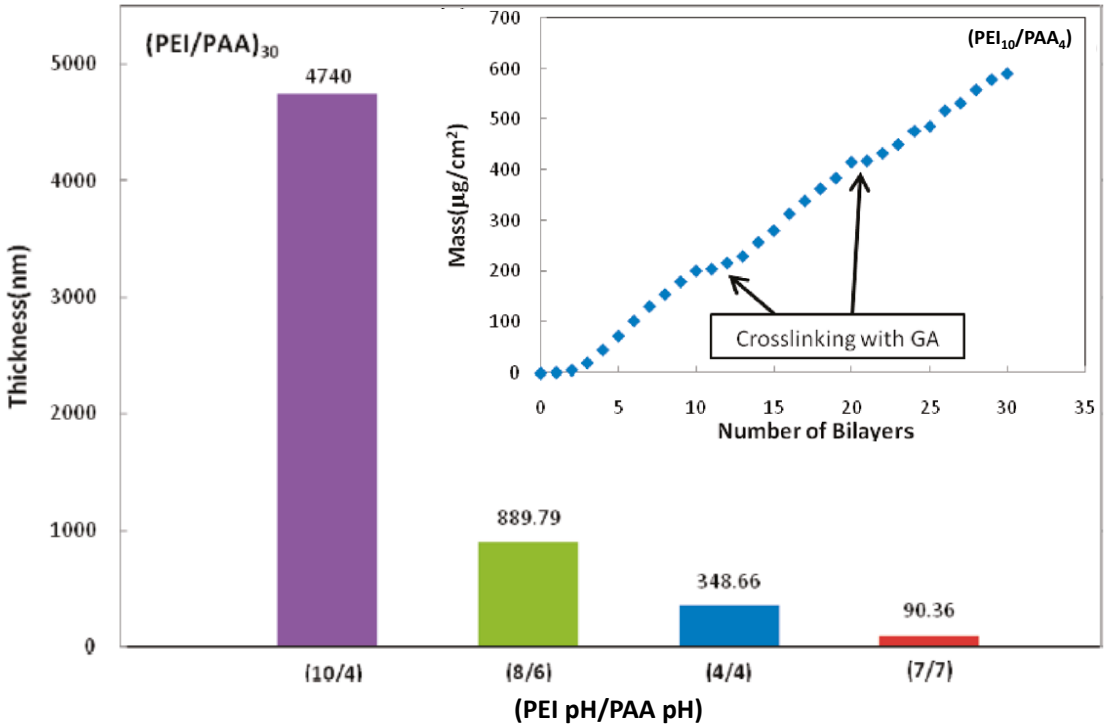

Figure 5. Film thickness of 30BLs PEI/PAA on silicon with varying pH combinations. The inset is mass as a function of deposited bilayers for 30 BLs of PEI10/PAA4 which highlights the reset film growth with crosslinking at 10 and 20BLs (from Ref. [28]).

Table 1. Oxygen permeability of PEI_{10}/PAA_4 assemblies on PET film at 23°C (Adapted from Ref. [28]).

Recipe	OTR[a] ($cm^3 \cdot m^{-2} \cdot day^{-1} \cdot atm^{-1}$)		Film Thickness (nm)	Permeability ($x10^{-16}$ $cm^3(STP) \cdot cm \cdot cm^{-2} \cdot s^{-1} \cdot Pa^{-1}$)	
	0% RH	100% RH		Coating[b]	Total
$(PEI_{10}/PAA_4)_{10}$	<0.005	<0.005	1080	<0.0006	<0.0096
$(PEI_{10}/PAA_4)_{10}$ + CL	<0.005	0.07	680	<0.0004	<0.0096
$(PEI_{10}/PAA_4)_8$	<0.005	0.61	451	<0.000048	<0.0096
$(PEI_{10}/PAA_4)_8$ + CL	<0.005	0.09	305	<0.000032	<0.0096
$(PEI_{10}/PAA_4)_6$	3.75	3.83	369	0.057	7.70
$(PEI_{10}/PAA_4)_6$ + CL	0.56	0.17	231	0.0032	1.15

[a]Coating permeability was decoupled from total permeability using a previously described method.[29]
[b]The low end detection limit for an Ox Tran 2/21 L module is 0.005 $cm^3 \cdot m^{-2} \cdot day^{-1}$.

4. Conclusions

Thin films, made of cationic, branched polyethylenimine and anionic sodium montmorillonite and poly(acrylic acid), were created using layer-by-layer assembly. These films were deposited on

silicon, Ti/Au, polystyrene, and poly(ethylene terephthalate) in an effort to comprehensively examine their properties. TEM confirms the platelet orientation and the nano brick wall structure that renders these polymer-clay films excellent oxygen barrier coatings. Thickness measurements based on ellipsometry reveal exponential growth of both the polymer-clay quadlayer films and all-polymer bilayer films. On 7-mil PET, only 4 quadlayers of PEI-PAA-PEI-MMT at 51 nm thick or a crosslinked 8 bilayers of PEI-PAA at 305 nm are necessary to achieve an oxygen transmission rate below the detection limit of commercial instrumentation (< 0.005 $cm^3 \cdot m^{-2} \cdot day^{-1}$). These two films,4QLs and 8BLs, exhibit the lowest thin film permeablilities ever reported for polymer-clay and all-polymer materials, respectively. These films provide an alternative to thin inorganic oxide coatings for food, pharmaceutical and flexible electronics packaging. Additional crosslinking, tailoring clay spacing, and increasing film clay content are currently being investigated as means to further improve the barrier behavior and environmental stability of these films.

5. REFERENCES

1. Ariga, K., J.P. Hill, and Q.M. Ji, *Layer-by-layer assembly as a versatile bottom-up nanofabrication technique for exploratory research and realistic application.* Phys. Chem. Chem. Phys., 2007. **9**(19): p. 2319-2340.
2. Decher, G., *Fuzzy nanoassemblies: Toward layered polymeric multicomposites.* Science, 1997. **277**(5330): p. 1232-1237.
3. Fu, J.H., et al., *Construction of antibacterial multilayer films containing nanosilver via layer-by-layer assembly of heparin and chitosan-silver ions complex.* Journal of Biomedical Materials Research Part A, 2006. **79A**(3): p. 665-674.
4. Dvoracek, C.M., et al., *Antimicrobial Behavior of Polyelectrolyte-Surfactant Thin Film Assemblies.* Langmuir, 2009. **25**(17): p. 10322-10328.
5. Kim, J.H., S.H. Kim, and S. Shiratori, *"Fabrication of nanoporous and hetero structure thin film via a layer-by-layer self assembly method for a gas sensor".* Sensors and Actuators B-Chemical, 2004. **102**(2): p. 241-247.
6. DeLongchamp, D.M. and P.T. Hammond, *"Highly ion conductive poly(ethylene oxide)-based solid polymer electrolytes from hydrogen bonding layer-by-layer assembly".* Langmuir, 2004. **20**(13): p. 5403-5411.
7. Yao, G.J., et al., *"Self-assembly and photovoltaic properties of multilayer films based on partially doped polyaniline and poly (4-carboxyphenyl) acetylene".* Journal of Polymer Science Part a-Polymer Chemistry, 2004. **42**(13): p. 3224-3229.
8. von Klitzing, R. and B. Tieke, *"Polyelectrolyte membranes".* Polyelectrolytes with Defined Molecular Architecture I, 2004. **165**: p. 177-210.
9. Dvoracek, C.M., et al., *"Antimicrobial Behavior of Polyelectrolyte-Surfactant Thin Film Assemblies".* Langmuir, 2009. **25**(17): p. 10322-10328.
10. Park, Y.T., A.Y. Ham, and J.C. Grunlan, *High Electrical Conductivity and Transparency in Deoxycholate-Stabilized Carbon Nanotube Thin Films.* Journal of Physical Chemistry C, 2010. **114**(14): p. 6325-6333.
11. Li, Y.C., J. Schulz, and J.C. Grunlan, *"Polyelectrolyte/Nanosilicate Thin-Film Assemblies: Influence of pH on Growth, Mechanical Behavior, and Flammability".* Acs Applied Materials & Interfaces, 2009. **1**(10): p. 2338-2347.
12. Li, Y.C., et al., *Flame Retardant Behavior of Polyelectrolyte−Clay Thin Film Assemblies on Cotton Fabric.* ACS Nano, 2010. **6**(4): p. 3325-3337.
13. Ploehn, H.J. and C.Y. Liu, *Quantitative analysis of montmorillonite platelet size by atomic force microscopy.* Industrial & Engineering Chemistry Research, 2006. **45**(21): p. 7025-7034.
14. Owens, D.K., *Mechanism of Corona-Induced Self-Adhesion of Polyethylene Film.* J. Appl. Polym. Sci., 1975. **19**(1): p. 265-271.
15. Zhang, D., Q. Sun, and L.C. Wadsworth, *Mechanism of corona treatment on polyolefin films.* Polym. Eng. Sci., 1998. **38**(6): p. 965-970.
16. Geddes, N.J., et al., *Surface Chemical Activation of Quartz-Crystal Microbalance Gold Electrodes - Analysis by Frequency Changes, Contact-Angle Measurements and Grazing Angle Ftir.* Thin Solid Films, 1995. **260**(2): p. 192-199.
17. Jang, W.S. and J.C. Grunlan, *Robotic dipping system for layer-by-layer assembly of multifunctional thin films.* Review of Scientific Instruments, 2005. **76**(10): p. -.

18. Gamboa, D., et al., *Note: Influence of rinsing and drying routines on growth of multilayer thin films using automated deposition system.* Review of Scientific Instruments, 2010. **81**(3): p. -.
19. International, A., *ASTM D3985 - 05 Standard Test Method for Oxygen Gas Transmission Rate Through Plastic Film and Sheeting Using a Coulometric Sensor*. 2005: West Conshohocken, PA.
20. Priolo, M.A., D. Gamboa, and J.C. Grunlan, *Transparent Clay-Polymer Nano Brick Wall Assemblies with Tailorable Oxygen Barrier.* ACS Applied Materials & Interfaces, 2010. **2**(1): p. 312-320.
21. Priolo, M.A., et al., *Super Gas Barrier of Transparent Polymer-Clay Multilayer Ultrathin Films.* Nano Letters, 2010. **in review**.
22. Roberts, A.P., et al., *Gas permeation in silicon-oxide/polymer (SiOx/PET) barrier films: role of the oxide lattice, nano-defects and macro-defects.* Journal of Membrane Science, 2002. **208**(1-2): p. 75-88.
23. Inagaki, N., S. Tasaka, and H. Hiramatsu, *Preparation of oxygen gas barrier poly(ethylene terephthalate) films by deposition of silicon oxide films plasma-polymerized from a mixture of tetramethoxysilane and oxygen.* Journal of Applied Polymer Science, 1999. **71**(12): p. 2091-2100.
24. Erlat, A.G., et al., *SiOx gas barrier coatings on polymer substrates: Morphology and gas transport considerations.* Journal of Physical Chemistry B, 1999. **103**(29): p. 6047-6055.
25. Mark, J.E., *Polymer data handbook*. 2nd ed. 2009, Oxford ; New York: Oxford University Press. vii, 1250 p.
26. Cussler, E.L., et al., *Barrier Membranes.* Journal of Membrane Science, 1988. **38**(2): p. 161-174.
27. Park, H.B. and Y.M. Lee, *Polymeric Membrane Materials and Potential Use in Gas Separation*, in *Advanced Membrane Technology and Applications*, N.N. Li, et al., Editors. 2008, John Wiley & Sons, Inc.: Hoboken, New Jersey. p. 633-669.
28. Yang, Y.-H., et al., *Super Gas Barrier of All-Polymer Multilayer Thin Films.* Macromolecules, 2011: p. null-null.
29. Roberts, A.P., et al., *Gas permeation in silicon-oxide/polymer (SiOx/PET) barrier films: role of the oxide lattice, nano-defects and macro-defects.* J. Membr. Sci., 2002. **208**(1-2): p. 75-88.